Crack Street: The Cycloidal Wake of a Cylinder Tearing through a Thin Sheet

A. Ghatak* and L. Mahadevan*,†

Department of Applied Mathematics and Theoretical Physics, University of Cambridge, Wilberforce Road, Cambridge, CB3 0WA United Kingdom

(Received 22 July 2003; published 21 November 2003)

When a cylindrical tool cuts through a thin sheet of a relatively brittle material, it leaves behind a visually arresting crack street in its wake, reminiscent of a vortex street in the wake of a cylinder moving through a fluid. We show that simple geometrical arguments based on the interplay of in-plane stretching and out-of-plane bending suffice to explain the cycloidal morphology of the curved crack. The coupling between geometry and dynamics also allows us to explain the "stick-slip"-like behavior of tearing and suggests that these oscillations should occur generically in the brittle fracture of thin solid films.

DOI: 10.1103/PhysRevLett.91.215507 PACS numbers: 62.20.Mk, 46.50.+a, 47.54.+r, 92.10.Rw

Despite enormous recent efforts to understand the stability and motion of cracks [1], there is no general theory capable of predicting the path of a crack as it moves through a three-dimensional solid. Thus one might imagine that if one considers the motion of a crack in a thin sheet capable of geometrically large deformations, the problem becomes essentially untractable. In fact, the vast separation of length scales actually simplifies the problem by clearly separating the statics and dynamics of the different modes of deformation. Therefore crack propagation in thin films offers a very different window into the mechanics and dynamics of fracture, both in the context of fundamentals and in processes involving thin films in materials science [2,3], impact engineering [4], and geophysics [5,6]. Here we address the unsteady dynamics and oscillatory morphology of a crack that forms in the wake of a relatively blunt tool used to cut through a thin brittle film, motivated by observations of the everyday chore of opening an envelope. If a knifelike letter opener is used, the result is a cleanly opened envelope with a single straight crack. If one uses a finger instead, the result is usually a rather raggedly torn envelope. This suggests that there is an instability that is controlled by the ratio of the tool (finger) diameter d to the sheet thickness h.

To investigate this phenomenon using a controlled experiment, we attach a thin sheet ($h = 40$–$50\ \mu$m) made of a relatively brittle material such as polypropylene with a low tearing strength (wrappers used to package audio and video tapes, compact disks, etc., all work very well because of their layered structure which makes them stiff to in-plane tensile forces but relatively soft in bending/out-of-plane shear) by clamping it to a long rigid rectangular frame (length l, width $w, h \ll w < l$) along its length, as shown in Fig. 1(a). A sharp notch centered along one of the free lateral edges is used as a nucleating site from where tearing is initiated by the tool, a rigid rod ($d \sim 0.25$–25 mm) of circular cross section with its axis perpendicular to the plane of the frame. The tool is attached to a motorized stage that can move parallel to the long axis of the frame at a uniform speed ($v_t \sim 0.25$–25 mm/s). When the aspect ratio $d/h < (d/h)_c$, a critical threshold, the crack in the wake of the tool is straight. However, when $(d/h) > (d/h)_c$, the straight crack loses stability to a spatiotemporal oscillatory mode of propagation, leaving behind a torn edge which suffers no permanent out-of-plane deformation [7] but is highly regular [Figs. 1(b)–1(e)]. The form of the torn edge is independent of the cross-sectional shape of the tool [8]; square, rectangular, and hexagonal cross-sectional tools all lead to similar shapes. More complex tear morphologies are also seen when the sheet is initially nonplanar and/or slack leading to interesting dynamical transitions shown in Fig. 1(f); we will not consider these any further, and instead focus on the quantitative description of the periodic states in Figs. 1(b)–1(e). The mechanism for the instability can be understood by considering the deformation of the sheet in response to the forces that the tool exerts on it. When the diameter of the tool is smaller than or comparable to the thickness of the sheet, the primarily planar sheet deformation leads to a stress profile that yields a maximum hoop stress just ahead of the tool so that the sheet tears linearly just ahead of the tool. At the other extreme, if the tool diameter is much larger than the thickness of the sheet with $h \ll d < w < l$, so that all the scales are relatively well separated, the motion of the tool causes the sheet to bend out of the plane as shown in Fig. 2(a). In this situation, the maximum stress that leads to rupture is no longer directly ahead of the tool but is instead at an angle to the direction of tool motion. If the maximum deflection of the sheet in the vicinity of the tool is denoted by ζ, the typical curvature induced in the sheet by the tool scales as ζ/d^2, so that the bending energy density $U_B \sim Eh^3\zeta^2/d^4$, where E is the Young's modulus of the material. The stretching strain due to bending scales as ζ^2/d^2 so that the stretching energy density $U_S \sim Eh\zeta^4/d^4$. Therefore, the ratio of the energy release rate in bending to that in stretching $G_B/G_S \sim U_B/U_S \sim \zeta^2/d^2$ [3] . Thus if the deflection of the sheet is larger than its thickness, the sheet prefers to tear by out-of-plane bending, while if the deflection is of the order of the thickness, the sheet ruptures via in-plane stretching.

When $d \ll h$, the geometry of interaction between the tool and the sheet leads naturally to a periodic transition from stretching to bending and back. At the beginning of a cycle, the crack tip is at its maximum lateral amplitude relative to the direction of the motion of the tool, so that the sheet is deformed primarily in the plane [Fig. 2(a)], causing it to stretch, until it eventually ruptures forming a crack that propagates at a speed that is much larger than the tool speed. Since the stress field far ahead of the tool is relatively small, the propagating crack slows down and comes to rest relatively quickly [9]. Once the tool catches up, it continues to tear the sheet, but now via a bending mode that is relatively cheap energetically. As this process continues, the crack tip moves in a direction perpendicular to the motion of the tool; the geometry of this motion automatically reduces the amount that the sheet has to bend to accommodate the tool motion until the crack tip is at a location corresponding to its mirror image (relative to the axis of motion in a frame attached to the tool). Further motion of the tool loads the crack in extension (mode I) and harks the beginning of the second half of a cycle. Evidence of the stretching and bending modes of failure can be seen by examining the tearing front under an optical microscope. In Fig. 2(b), we see that close to the crest of the wavy pattern, i.e., from A to B the edge of the crack is nearly perpendicular to the sheet, indicating failure under in-plane stretching, while the edge of the crack is slanted from B to C indicating failure due to out-of-plane bending/shear.

The shape of the torn edge is particularly easy to understand in the extreme case when all the lengths in the problem are asymptotically far apart, and the crack is assumed to propagate quasistatically (realizable using a feedback control loop to prevent the crack from accelerating as it first starts in the stretching mode). Then the crack tip will trace out the path of a point on the circumference of the tool which moves at constant velocity in a

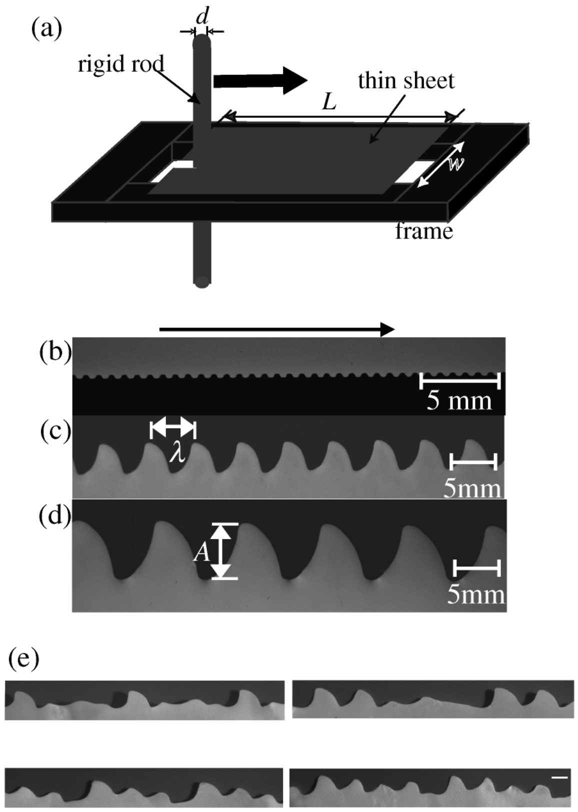

FIG. 1. Experimental setup and tear morphology. (a) Schematic of the experiment in which a rigid rod is driven transversely through a thin sheet of plastic (length $l = 230$ mm and the width $w = 30$ mm) attached laterally to a rigid frame. The sheet is stretched slightly so that it does not sag between the edges of the frame. (b)–(e) Typical tearing patterns as a function of the sheet thickness h and tool diameter d. (b) $h = 40\ \mu$m, $d = 0.25$ mm; (c) $h = 50\ \mu$m, $d = 3$ mm; (d) $h = 40\ \mu$m, $d = 8$ mm. (e) If the film has some lateral slack induced by bringing the lateral edges closer (so that $\Delta w = 2.5$ mm), and a rigid rod of diameter $d = 3$ mm is driven through the sheet at a speed $v_t = 5.3$ mm/s, we see the evolution of periodic patterns, starting with a single tooth pattern that gives way to multiteeth patterns and eventually leads to the continuous cycloidal patterns that are seen when there is no slack in the sheet. The scale bar corresponds to 1 cm.

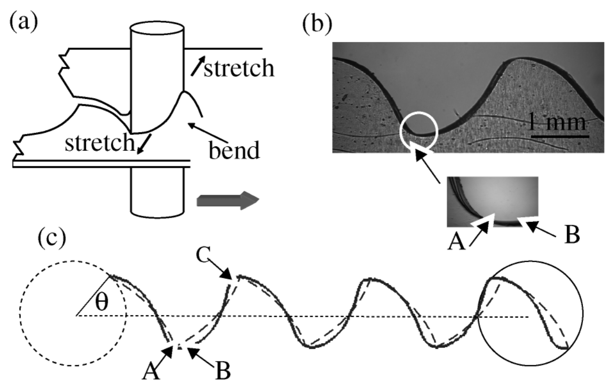

FIG. 2. Geometry and mechanics of tearing. (a) The sheet tears by two different mechanisms: in-plane-stretching and out-of-plane bending. The first mechanism is operative at the beginning of each cycle, while the second takes over during the rest of the cycle. (b) The edge of the crack close to the crest is perpendicular to the sheet, signifying ripping of sheet by in-plane-stretching. Away from the crest it is slanted, signifying out-of-plane shearing due to bending of sheet. (c) The crack wake left behind the tool (solid line) showing the region corresponding to in-plane stretching (A to B) and out-of-plane bending (B to C). The tearing path is reasonably well described by a series of cycloidal arcs [$x = R(\theta - \sin\theta)$; $y = R(1 - \cos\theta)$; $R = 1.15d/2 = 0.575d$; $\theta \in [-42°, 42°]$] which would correspond to the ideal situation when the crack tip hugs the tool, tracing out a point on its circumference. Here the sheet thickness, $h = 50\ \mu$m, the tool diameter $d = 3$ mm, and the tool speed $v_t = 5.3$ mm/s.

given direction. For a tool with a circular cross section, the path of a point on the circumference of the circle that rolls along a plane defines a cycloid, represented parametrically as

$$x = \frac{d}{2}(\theta - \sin\theta), \qquad y = \frac{d}{2}(1 - \cos\theta), \tag{1}$$

where θ is the angular position of the crack tip relative to the direction of tool motion. Thus, we might expect that the crack tip follows an arc of a cycloid over each half-cycle of tearing. Figure 2(c) shows that this is a good approximation and the small deviations from the cycloidal path that arise are due to finite size and dynamical effects. Quantitatively, the experimentally fitted cycloid is characterized by a circle of radius $\alpha d/2(\alpha > 1)$, and is limited to angular variations with $\theta \in [-\beta\pi/2, \beta\pi/2]$, $(\beta < 1)$. The parameters α, β can be determined only via a detailed stress analysis that accounts for the complex geometry of loading. Nevertheless, the geometrical interpretation allows us to immediately infer that the amplitude A and wavelength λ should both scale linearly with the tool diameter d. In Figs. 3(a) and 3(b), we show that this is indeed the case in the unstable tearing regime. Furthermore λ, A are independent of the tool speed v_t over almost 2 orders of magnitude (0.25–25 mm/s).

The alternation between stretching and bending deformations also has dynamical implications, which we study by tracking the crack tip using high-speed photography (500–5000 fps). In Fig. 4(a), we show the position of the crack tip as a function of time and see that in each cycle the crack moves in two stages; very rapidly at first and then very slowly, reminiscent of frictional stick-slip behavior. This is clearly seen in Fig. 4(b), where we show the crack tip velocity v as a function of time and see the presence of two vastly different velocities, the tool speed v_t and the maximum crack speed $v_c(\gg v_t)$ which is a function of the material properties and the geometry of the experiment. However, the maximum speed of the crack, $v_c \sim 1$ m/s is much smaller than the inertial wave speeds in the medium $v_i \sim (E/\rho)^{1/2} \sim 3 \times 10^3$ m/s (and also much less than the Rayleigh wave speed), suggesting that local dissipation mechanisms lead to the slowing down of the crack. In terms of a simple viscous model for the dissipation close to the crack tip during in-plane tearing, the rate of dissipation scales as $\mu(v_c/h)^2h^3$ where μ is the effective "viscosity" of the medium [10]. The driving power due the elastic stresses which scales as $E\epsilon^2 dhv_c$ where ϵ is the typical strain in the neighborhood of the tool. Balancing the driving power with the dissipation rate yields

$$v_c \sim E\epsilon^2 d/\mu. \tag{2}$$

Substituting in typical values for the experimental parameters with $E \approx 10^{10}$ Pa, $d \approx 10^{-2}$ m, $\epsilon \approx 10^{-1}$,

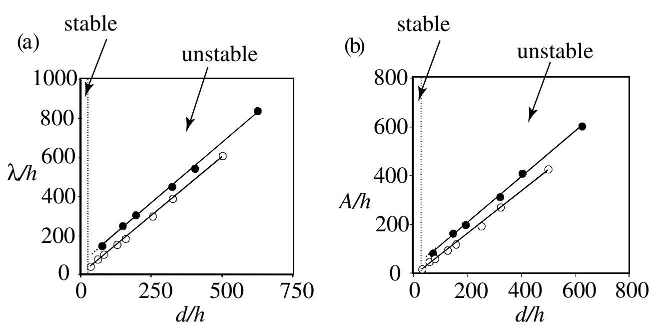

FIG. 3. Wavelength and amplitude of the wake. (a) Below a critical value of the aspect ratio of the tool, $(d/h)_c \sim 30$, the crack is straight and stable, while above it, the crack is unsteady and curved. The scaled wavelength λ/h varies linearly with the scaled tool diameter d/h. The closed and open symbols represent data for sheets of thickness 40 and 50 μm, respectively. The solid line is given by $\lambda/h = (1.22 \pm 0.01)d/h$. (b) The dimensionless amplitude A/h of the pattern also varies linearly with d/h. Closed and open symbols represent films of thickness 40 and 50 μm, respectively, and the solid line is given by $A/h = (0.9 \pm 0.03)d/h$. For the 40 μm film, the dotted line indicates a transition region, in which tearing can be both stable and unstable.

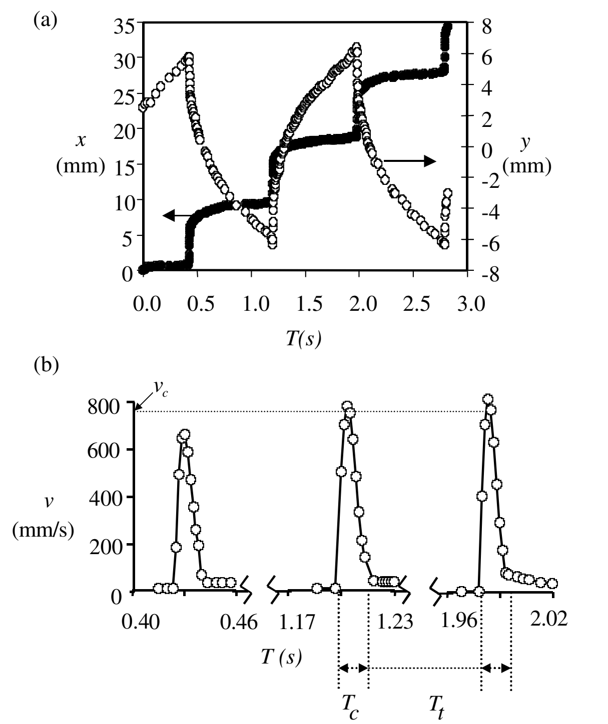

FIG. 4. Stick-slip dynamics of tearing. (a) Position of the crack tip as a function of time. The filled and open symbols correspond to the x and y coordinates of the tip, respectively. Here $d = 12$ mm, $h = 50$ μm, and $v = 12.5$ mm/s. (b) Velocity of the tip v_c as a function of time. Two different times scales of crack propagation (T_t and T_c) can be identified in this figure. $T_t \sim d/v_t$, is the slow time scale associated with the tool speed, while $T_c \sim d/v_c$ is the fast time scale associated with the maximum intrinsic crack speed in the sheet v_c.

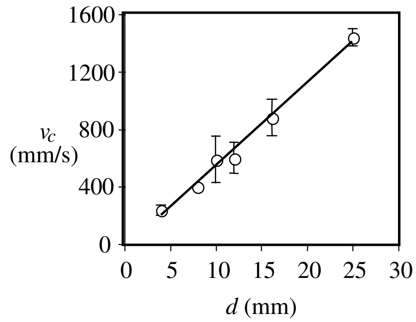

FIG. 5. The maximum crack speed v_c increases linearly with tool diameter d(2–25 mm) and is independent of the tool speed over the entire range of speeds tested, consistent with (2). The solid line is given by $v_c = 58d - 33.4$. The finite horizontal intercept suggests that if the diameter of the tool is below a critical value, the stick-slip behavior will give way to steady tearing, qualitatively consistent with observations.

$\mu \approx 10^6$ Pa s, we find that $v_c \approx 1$ m/s, in agreement with our measurements. To test the dependence of the maximum crack speed on the tool size, we varied the latter by a factor of 5. In Fig. 5, we show that the maximum crack speed $v_c \sim d$ consistent with (2).

The crucial simplifying feature of our system has been the geometry-induced separation of deformation modes (into stretching and bending) that allows us to qualitatively understand the morphology and dynamics of forced tearing in thin films. Although a detailed analysis is clearly required in order to understand such questions as the transition to oscillatory tearing and the angle of tear initiation, as we move away from the onset of the instability, the separation of scales makes the asymptotic analysis ever easier. Naturally therefore, these ideas may be relevant to problems involving extremes in scale separation, as in geology, a subject to which we turn briefly.

On Earth, in the polar regions, sometimes ice sheets are driven past grounded icebergs by winds and ocean currents, and lead to a cycloidal crack morphology over a scale of many kilometers [5], similar to that seen in our laboratory experiments. Indeed, the mechanism of cracking should be identical to the one we have presented, although there are currently no dynamic observations of these processes. This might also help to explain the nature of finger rafts, an unusual morphology of ice sheets with fingerlike projections that interleave each other [6]; it is likely that these are just the remnants of an ice sheet torn by an iceberg. Indeed, this interplay between geometry and dynamics suggests that generically crack propagation in thin films involving bending and stretching will typically lead to stick-slip oscillations.

We thank Peter Wadhams for educating us about the mechanics of ice sheets. A. G. and L. M. acknowledge the support of the U.S. National Institutes of Health and the Office of Naval Research.

Note added in proof.—While going to press, we became aware of other experiments studying the same phenomena [11].

*Current address: Division of Engineering and Applied Sciences, Harvard University, Cambridge, MA 02138, USA.

†Email address: lm@deas.harvard.edu

[1] K. Broberg, *Cracks and Fracture* (Academic Press, London, 1999).

[2] J.W. Hutchinson and Z. Suo, Adv. Appl. Mech. **29**, 63–191 (1992).

[3] C.Y. Hui, A.T. Zhender, and Y.K. Potdar, Int. J. Fract. **93**, 409–429 (1998).

[4] *Structural Crashworthiness and Failure*, edited by N. Jones and T. Wierzbicki (Elsevier Science, Amsterdam, 1993).

[5] S. Sandven and O. M. Johannessen, J. Photogramm. Remote Sensing, **48**, 2–18 (1993)

[6] A. Kovacs, in *Sea Ice, Proceedings of an International Conference*, edited by T. Karelsson (Natl. Res. Council, Reykjavik, Iceland, 1972), pp. 276–295.

[7] The instability arises via a Hopf bifurcation as is to be expected on the grounds of symmetry, so that the relationship between the amplitude and the wavelength is nonlinear close to the onset of the instability. However, we will focus on the regime far from onset where the problem becomes much simpler.

[8] The tool shape is not important since in the real experiment, which is displacement controlled, the crack tip is always slightly ahead of the tool. Therefore, the detailed shape of the tool is not "felt" by the bent sheet when all the length scales in the problem are far from each other.

[9] The stress field generated by the tool decays over a characteristic length comparable to the tool diameter d. The rapid phase of crack propagation leads to crack motion over a distance δd, $\delta \leq 1$.

[10] The rheology of the material is of course much more complex that than of a Newtonian fluid so that the viscosity must be interpreted in terms of a frequency-dependent loss modulus.

[11] B. Roman, P. M. Reis, B. Audoly, S. De Villiers, V. Viguié, and D. Vallet, "Oscillatory fracture paths in thin elastic sheets," C. R. Mécanique (to be published).